Available online at www.sciencedirect.com

ScienceDirect

Procedia Structural Integrity 24 (2019) 40–52

Structural Integrity Procedia

www.elsevier.com/locate/procedia

AIAS 2019 International Conference on Stress Analysis

# A comparison of state-based peridynamics and solid mesh to SPH conversion techniques to reproduce fragmentation of a ceramic tile subject to ballistic impact

Riccardo Masoni[a], Andrea Manes[b]*, Marco Giglio[a]

[a]*Politecnico di Milano, Department of Mechanical Engineering, via la Masa, 1, 20156, Milan, Italy*

**Abstract**

This paper presents a comparison of two present meshfree approaches for modelling brittle material in case of ballistic impact, where extensive cracking and fragmentation is present. These phenomena are very unfeasible to simulate with a standard Lagrangian technique thus alternative methods have been considered in the last years. A comparison between two methods is the main aim of the present article. Smoothed Particle Hydrodynamics (SPH) is an almost consolidated method that exploit the description of a continuum by means of discrete elements whose properties are "smoothed" by a Kernel Function. In this paper a procedure that exploits the transition from finite elements (FE) to SPH particles, following the onset of an erosion criterion is used. This approach and its results are then compared to the recent state-based Peridynamics. Peridynamics method is based on integral equation and allow a direct application to discontinuities and fractures. The results from both methods are critically compared with experimental data and show that the damage morphology is reproduced similarly by both approaches; however less computation efforts are required when peridynamics are used.



*Keywords:* meshfree; impact; brittle material;

* Corresponding author. Tel.: +39-02 2399 8630; fax: +39-02 2399 8263.
*E-mail address:* andrea.manes@polimi.it


10.1016/j.prostr.2020.02.004

## 1. Introduction

Ceramic materials are widely employed in multilayer ballistic armours in personal, vehicles and aircraft protections. Their widespread use is mainly related to their unique mechanical properties. The main advantages of this class of materials is high hardness and stiffness, combined with a favourable efficiency-weight ratio: when a ceramic plate is impacted by a projectile, it erodes and shatters the impactor into pieces, significantly decreasing its penetrating capabilities. However, the defeat of the impactor also leads to a significant fragmentation of the ceramic tile. The failure mechanism of impacted ceramic materials is very complex and involves several mechanisms including radial cracking, cone cracking and comminution (due to microcracking). Thus, a lightweight and efficient armor system is generally composed of a hybrid system with a hard-ceramic strike face and a soft and ductile backing. The backing material is usually made of composites (e.g. Kevlar) or metal alloys, and its role is to contain the fragments of the ceramic and the projectile and to absorb the residual kinetic energy of the various pieces. The combination of ceramic and backing material provides a lightweight protection, especially in comparison with equivalent protection made of ballistic steel.

Ballistic impact is a highly impulsive loading: when the projectile impacts the ceramic target, shock waves are generated. They are reflected on the free surfaces as tensile stress waves and they cause material fracturing when the magnitude of the tensile stress wave is greater than the dynamic tensile strength. Radial cracks are initially nucleated at the back face of the plate, in correspondence to the projectile impact area, then they propagate from the bottom to the strike face Krishnan *et al* (2010). Circumferential or ring cracks are also generated, as well as conical and lateral cracks if the target is thick. Before the projectile begins to penetrate the target, a highly damaged zone is generated in front of the projectile path. This volume of material is shaped as a cone and known as Mescall zone: it is constituted of highly comminuted and pulverized material, Council *et al* (2011), that is ejected at high velocity from the back and the strike face. Moreover, bigger fragments of material are formed from the interaction of macro-cracks and detached from the main body. Damage morphology characteristics are dependent on many different factors, for example the tile thickness, shape and mechanical properties, the shape of the impacting projectile, the material, the impact angle and the velocity. Very important is also the presence of a backing or a covering material, as well as constrains eventually applied to the ceramic target.

Experimental ballistic tests are therefore subject to highly variable results additionally being expensive and time consuming. Numerical simulation can be a very useful tool in the design process of protection systems where ceramic material are involved. The use of virtual tests can be relevant in the design phase in order to fit the capability of the protection to the required actual condition and to increase the understanding of the physical phenomena that drive the impact event. However, the fragmentation phenomenon, typical of an impact against ceramic, is difficult to model numerically with traditional tools: Finite Element (FE) Lagrangian approaches. Different phenomena must be modelled in the case of impacts, such as penetrations, large deformations, creation of free surfaces (crack openings), material separation and fragmentation. Lagrangian mesh-based approaches exhibit decreasing accuracy with increasing mesh distortion, and they do not directly provide means to model crack nucleation and propagation, large fragmentation related to material failure. These limitations can be avoided with alternative and/or additional techniques, each one with their own advantages and disadvantages. Exploiting element erosion in Lagrangian approaches, when a finite element property satisfies a predefined criterion, the mesh element is usually removed from the simulation. In Tasdemirci and Hall (2007) the damage onset in multilayer composites materials, made of a ceramic layer and composite backing is studied. An erosion criterion based on the effective plastic strain is used to model damage and material failure in the ceramic layer. The impact of an armor-piercing projectile against a hybrid lightweight armor was simulated in Grujicic *et al* (2007): the first layer of the armor is an alumina tile reinforced with fiber glass; impact was modelled with FE and an erosion criterion was used based on the instantaneous geometrical strain. In Council *et al* (2011) a ceramic armor with an aluminum backing was subjected to ballistic impact: an erosion criterion was used for the projectile and for the two armor layers. The critical erosion strain was updated for each mesh size of the model. One of the main issues highlighted in these studies is the strong dependency on mesh size and type: crack paths can be sensitive to mesh texture and alignment, as discussed in Madenci and E. Oterkus (2014). When damage or failure is included, small elements can erode before larger elements, Schwer (2011). Moreover, element erosion causes non-physical mass loss. Better results can be obtained using improved erosion algorithms that try to reduce the mesh influence on the results, in a process called mesh regularization. The basic principle is to average

certain material variables between elements close to each other: this treatment is thus nonlocal, meaning that the state of a given mesh element is influenced by other elements not immediately adjacent. In Eringen (2002) a nonlocal averaging of displacement gradients was performed, while in Schwer (2011) the averaging process regarded failure and damage values.

Cohesive elements were used successfully to model extended fragmentation of brittle materials in the works by Camacho and Ortiz (1996) and Mota *et al* (2003). More recently, cohesive elements were used successfully with a hybrid discontinuous Galerkin formulation Radovitzky *et al* (2011).

Node-Splitting is a recent and innovative 3D technique, implemented in the FE code IMPETUS Afea® Solver. This method allows cracks to propagate between elements: a failure criterion is used to determine when an element should split in two smaller elements. Note that the element is not deleted, so in general bigger elements can be used with respect to the traditional erosion approach. In Olovsson *et al* (2015) the simulation of the Taylor impact test of a fused silica bar reproduced the brittle failure as in experimental tests. In Moxnes *et al* (2015) the results obtained for the brittle fragmentation of a steel expanding warhead casing agreed with experimental evidence.

SPH elements are often used in the literature to model brittle material fragmentation in ballistic impacts: mesh free methods present in fact several advantages over Lagrangian approaches. In particular they can handle easily large deformations, since they do not need predefined connections between nodes. The small fragments generated by the impact are well reproduced by these elements and they are able to resist further to the advancement of the impactor. In high-velocity impacts SPH elements can correctly reproduce the debris cloud created. In Ma *et al* (2009) the SPH method was used and validated with experimental data which were compared with the results, obtained with element erosion, demonstrating the superiority of the SPH approach. In Michel *et al* (2006) a high-velocity impact on a thin brittle target modelled with SPH was simulated. The resultant morphology and fragments distribution were validated with experimental data. Again, SPH elements were used in Nordendale *et al* (2013) to model a concrete armor subject to ballistic impact.

Recently, different coupled FEM-SPH approaches have been successfully employed: they have the advantage of mitigating SPH related problems, such as tensile instability and high computational cost, and often improve the accuracy and quality of the simulation. If the impact damage is localized only in a small area of the target, then the SPH elements can be used only for that part of the domain, while the rest is modelled with FE. In this case FE and SPH are coupled by an appropriate algorithm, Zhang and Qiang (2011). This approach was used in Zhang *et al* (2011) with a steel armor. A different method, more suitable for ceramic materials, since they exhibit extensive cracking and fragmentation, consists of the conversion during the simulation of eroded FE into SPH particles. These particles inherit the same properties of the converted elements and are able to interact with the rest of the computational domain. In Kala and Husek (2016) this approach was named “improved element erosion” and was used to model the ballistic impact against a concrete material and validated with analytical calculations. In Bresciani *et al* (2016) it was used to model the fragmentation of an alumina (spelling) plate.

Peridynamics is a nonlocal reformulation of solid continuum equations, and it is therefore suitable to model the presence of discontinuities, such as cracks. Its governing equations are based on a spatial integration, while the classical continuum theory uses partial differential equations with spatial derivatives that are not valid on discontinuities. Since it is a nonlocal approach, the state of a material point is influenced by a set of points located within a finite distance. Peridynamics method was first introduced by Silling (2000) and subsequently further improved resulting in state-based peridynamics, a more general and refined theory, introduced by Silling *et al* (2007) . It is generally implemented as a mesh free method, so that the problem domain is discretized by nodes with a given volume, similarly to SPH. A great advantage of peridynamics is that material damage is part of its constitutive laws and allows cracks initiation and propagation realistically and within the peridynamics framework, Madenci and Oterkus (2014). It has been used successfully to simulate impacts and crack propagation on brittle materials by Bobaru *et al* (2012), Bless and Chen (2010) and Hu (2012).

Also, the Discrete Element Method has been applied successfully to model ceramic materials. In Wittel *et al* (2008) the brittle fragmentation of spheres impacting a hard surface was studied, with a focus on crack generation and fragment size distribution. The impact of steel balls against hot-pressed alumina (spelling) disks was tested both experimentally and numerically in Kudryavtsev and Sapozhnikov (2016). The numerical parameters were calibrated by using an inverse method; results accurately reproduced the experimental results.

In this paper FE-to-SPH and state-based peridynamics approaches are used in order to assess their behaviour in simulating an impact against ceramic. An experimental test from the literature, Nemat-Nasser *et al* (2002), is used for the assessment of the numerical models. An evaluation of the produced damage morphology is performed comparing the two methods. Peridynamics presents some advantages, in particular on the required material data and model calibration. Obtained results are similar, indicating a similarity between peridynamics and SPH. However, the computational time required for the peridynamics model is around 70% less than the FE-SPH model.
The article is divided into three (or four) sections. Section 2 introduces the experimental test that is used for the comparison and assessment of the modelling approaches. Subsequently the numerical models are described in Section 3 with separate sub-sections for SPH and peridynamics. Finally, the results obtained, and the techniques employed are compared and discussed.

## 2. Experimental data

Even if the actual protections are hybrid systems, an investigation of the bare ceramic is of interest especially with regards to defining and assessing predictive models. The possibility to investigate only the behaviour of ceramic material during impact events allows a more in-depth definition of a reliable predictive approach. In fact, the simulation of a complete hybrid protection implies a detailed investigation of both the constituents and their interaction thus making the task very complex. This work is focused on the fragmentation process of the ceramic material, thus the experimental test selected is performed on bare alumina plates without any backing and with minimal constraints.

In Nemat-Nasser *et al* (2002) a single-stage gas gun was used to test different ceramic materials. In the test selected, the target plate was made of a commercial high purity alumina used for armors, namely Coors AD995 CAP3, and of the dimensions 100.8x100.8x12.7 mm. No covering or backing materials were present. The tile rested on four support pins at its corners, held in place by rubber bands. The impactor was a blunt cylinder made of the tungsten heavy alloy WHA, containing nickel 5% and iron 2%, with a diameter of 6 mm and a length of 20 mm.

Data available for the ballistic test, Table 1, includes the impactor velocity and mass, before and after the impact. Moreover, two pictures of the specimen, one of the strike face and one of the back face, allow to validate the numerical results in terms of damage morphology of the plate.

Table 1. Experimental results from Nemat-Nasser *et al* (2002)

| | |
|---|---|
| Impactor Impact velocity | 903.9 [m/s] |
| Impactor Exit velocity | 682 [m/s] |
| Mass of the impactor | 10.6 g |
| Residual mass of the impactor | 6.4 g |
| Front face: number of radial cracks | 17 |
| Front face: equivalent radius | 22 mm |
| Back face: number of radial cracks | 19 |
| Back face: equivalent radius | 29 mm |

The ceramic plate fails through a combination of different processes visible in the *post-mortem* pictures. A quantitative analysis of the selected morphological features was performed in order to use the data to calibrate and validate the numerical models. For both faces the number of radial cracks formed was counted, as well as the dimension of the hole left on the surface, expressed as an equivalent radius. Indicative results are reported on Table 1. The left hole on the back face is bigger than the front face due to the formation of the fracture cone.

## 3. Numerical models

### *3.1.* SPH *approach*

With this approach the target is initially modelled with FE, thus it can be meshed with traditional tools. FE are more efficient from a computational point of view with respect to SPH when they have to handle small deformations. Moreover, this allows the reduction of computational time by using SPH elements only in case they are really needed. The commercial code LS-DYNA® is used, since it has the conversion method of FE to SPH already implemented with the card DEFINE_ADAPTIVE_SOLID_TO_SPH.

Only one fourth of the tile and projectile is modelled, taking advantage of the model's symmetry, see Figure 1. Both the projectile and the ceramic tile are modelled with 8-node hexahedrons with one point of integration. A regular mesh is used for the tile, without any impact-zone mesh refinement.

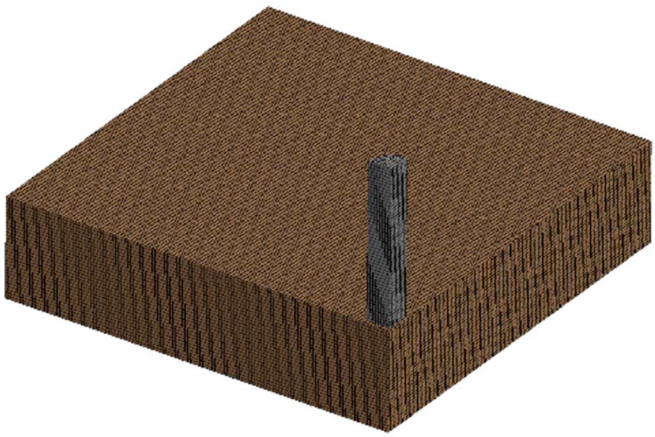

Fig. 1. The model for the SPH approach

This choice was made for multiple reasons: the target erosion is not only localized near the impact area, since multiple cracks propagate along the whole panel and the erosion process is mesh dependent thus the cracks paths can be influenced by a non-regular mesh. Furthermore, the distribution of the SPH particles should be as regular as possible to avoid consistency issues, Zhang and Qiang (2011), and the formation of particle clusters that can affect crack propagation, Zhang *et al* (2011). A mesh convergence analysis has therefore been performed and is discussed.

Appropriate symmetry boundary conditions are defined in the model. The card SPH_SYMMETRY_PLANE is used to define two symmetry planes for the particles. The projectile is constrained to translate only along the normal impact trajectory and its initial velocity is set to 903.9 m/s, as in the experimental test. Different possible support conditions for the tile were considered: the projectile residual velocity and the damage morphology differences are negligible in each case. In the end, the target was modeled as unconstrained, since this reflected the experimental conditions more accurately.

A study of the different fragmentation models available for the projectile was based on the techniques presented in Bresciani et al (2016). In one model the impactor was modelled with FE and an erosion criterion. In this case most of the projectile elements were eroded, incorrectly simulating the shattering into pieces described in the experimental tests and making the contact with the target discontinuous. A second model was developed using the FE-SPH conversion technique also for the projectile. Also, in this case the fragmentation of the projectile was limited, but the mass was conserved. Finally, in the most detailed model, as well as the most computationally demanding, the projectile was composed of many pre-fragmented hexahedral pieces bonded together by a cohesive law: in this case the projectile showed a good fragmentation into pieces. In all the tests performed the damage morphology of the ceramic tile was similar to the one obtained with a rigid projectile, and also the residual velocity of the impactor. The computational

time needed was definitely higher in the cases where the projectile was deformable. Since this research was mainly focused on the fragmentation of the ceramic plate, in order to reduce the computational time while still producing realistic results, the projectile was modelled as a rigid body.

The constitutive model used for the ceramic tile was the Johnson-Holmquist 2. The model parameters are reported in Table 2: the material properties were obtained from Kala and M Husek (2016) and Bresciani *et al* (2016).

Table 2. Coors AD995 CAP3 ceramic tile: Johnson-Holmquist 2 model parameters, Kala and M Husek (2016), Bresciani *et al* (2016)

| | |
|---|---|
| Density | 3900 [kg/m$^3$] |
| Elastic modulus | 390 GPa |
| Shear modulus | 152 GPa |
| Poisson's ratio | 0.22 |
| Intact strength coefficient | 0.93 |
| Fractured strength coefficient | 0.31 |
| C strain rate coefficient | 0 s$^{-1}$ |
| N Intact strength exponent | 0.6 |
| M fractured strength exponent | 0.6 |
| Normalized max fractured strength | 0.2 |
| Hugoniot Elastic Limit | 19 GPa |
| Pressure at HEL | 1.46 GPa |
| Bulking factor | 1 |
| Elastic bulk modulus | 220.24 GPa |
| 2$^{nd}$ EOS coefficient | 0 |
| 3$^{rd}$ EOS coefficient | 0 |
| Damage parameter 1 | 0.005 |
| Damage parameter 2 | 1 |

A contact of the type ERODING_SURFACE_TO_SURFACE was defined between the impactor and the plate. The contact between the generated SPH particles and the projectile was defined using a node to surface contact with the option SOFT=1. The contact between the SPH and the ceramic plate was defined automatically by the software.

The FE were converted to SPH particles when an erosion criterion was satisfied. To reduce the computational time, one element was converted to only a single particle, which inherited the eroded element properties (*e.g.* mass, momentum, internal energy). Two different erosion criteria were studied, one based on the effective total strain and one on the effective plastic strain.

The effective total strain was defined as, using an index notation:

$$\epsilon_{eff}^{tot} = \sqrt{\frac{2}{3}\epsilon_{ij}^{tot}\epsilon_{ij}^{tot}} \tag{1}$$

Where $\epsilon_{ij}^{tot}$ is the sum of the elastic ($\epsilon_{ij}^{e}$) and plastic ($\epsilon_{ij}^{p}$) part of the deviatoric strain tensor:

$$\epsilon_{ij}^{tot} = \epsilon_{ij}^{e} + \epsilon_{ij}^{p} \tag{2}$$

The effective plastic strain was calculated using only the plastic part of the total deviatoric strain tensor:

$$\epsilon_{eff}^{p} = \sqrt{\frac{2}{3}\epsilon_{ij}^{p}\epsilon_{ij}^{p}} \tag{3}$$

Different analyses were carried out as a function of the critical strain and mesh size. The results were analyzed in terms of capability to reproduce experimental results and evidence. The residual velocity of the projectile was considered for convergence studies as well as the number of radial cracks formed and the size of the comminution cone. The model was further verified by checking the energy ratio value during the simulation. The energy ratio was defined as the ratio of the total energy (at a given time) over the initial total energy plus external work (external work includes work done by applied forces and pressures as well as work done by velocity, displacement or acceleration boundary conditions). The energy ratio should be close to 1 during the entire computation in order to preserve the energy balance,

Starting from the effective total strain criterion, the chosen critical value of 6% effective total strain was used to trigger the element conversion from FE to SPH. This value provided a good ratio between the results and the computational time and was also used in similar cases in the literature, Feli and Asgari (2011), Bresciani *et al* (2016). However, the residual velocity of the projectile was not greatly affected by variations in the critical value. A mesh size convergence study was also performed showing that the residual velocity and damage morphology (number of radial cracks) converged for mesh sizes below 0.5 mm. As expected, in the volume close to the impact point a large number of elements was converted to SPH, but not all of them. Upon a closer observation of the SPH particle (or eroded elements) distribution near the impact, multiple cracks were visible to have developed inside the tile and medium sized fragments were formed, see Figure 3. The SPH particles in the area close to the projectile can be interpreted as the pulverized material ahead of the projectile tip. Some bigger fragments of material are outlined in blue; they are almost detached from the tile's principal body due to crack propagation.

As far as effective plastic strain criterion is concerned, a series of simulations were run using different values, but the mesh size was fixed at 0.4 mm. The results show that the residual projectile speed is not much affected by the parameter change, as well as the energy ratio maximum value. However, results obtained with different values of effective plastic strain criterion showed different behaviour in the fragmentation of the tile and the energy ratio. An effective plastic strain of 15% provided an acceptable damage morphology, and a relatively limited energy ratio maximum value. However, the mass increase at the end of the simulation was excessive (24%) and the energy ratio peak reached the value of 1.6 (thus energy is being introduced artificially).

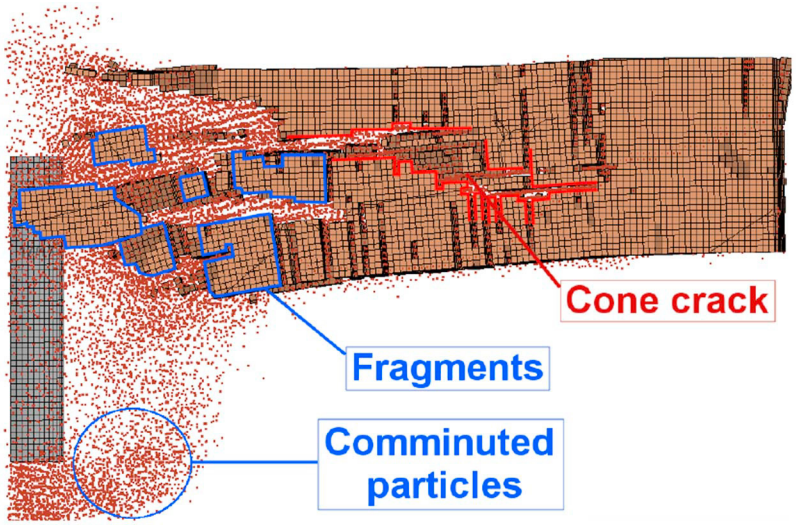


.

Fig. 2. Section view of the analyses that uses the total strain criterion for the conversion from FE to SPH

In Table 3 the values used for the final model are indicated, whereas in Figure 3 a comparison (experimental numerical) of the damage morphology for SPH approach is reported. The number of radial cracks and the size of the crater present on front and back surface were measured.

Table 3. SPH approach, main results from the models

| | Effective total deviatoric strain | Effective plastic deviatoric strain |
|---|---|---|
| Critical strain | 6% | 15% |
| Mesh size | 0.4 mm | 0.4 mm |
| Residual velocity | 628 m/s | 654 m/s |
| Energy ratio (final) | 1.04 | 1.24 |
| Mass increase | 13.4% | 23.5% |
| # Radial cracks front | 4 | 28 |
| # Radial cracks back | 20 | 12 |
| Eq. radius front | 13 mm | 24 mm |
| Eq. radius back | 27 mm | 29 mm |

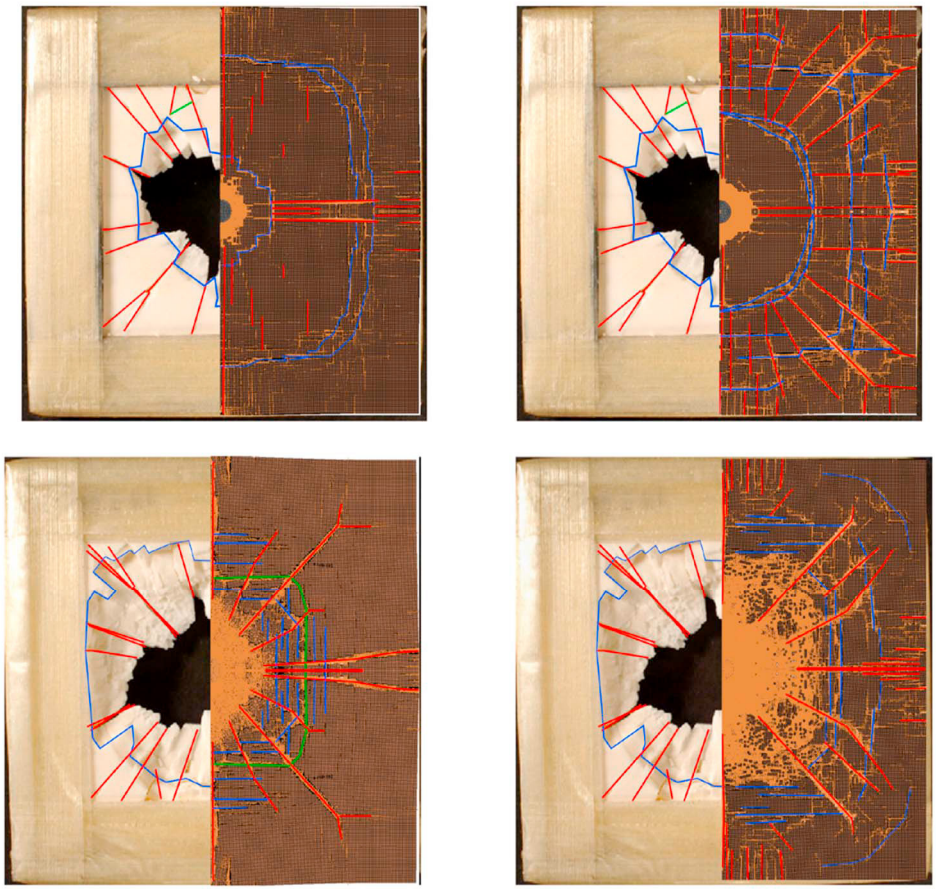

Fig. 3. Comparison of the damage morphology for SPH approach, experimental figure from Nemat-Nasser *et al* (2002): UPPER panels-front face, total strain (left), plastic strain (right), LOWER panels - back face, total strain (left), plastic strain (right)

A further validation was performed to compare also the numerical tensile stress wave speed with the experimental wave showing good matching.

A possible explanation of the mass increase can be related to the conversion to SPH of the hexahedron elements. They feature a lumped diagonal mass, where each node has assigned one eight of the element's mass. When an element sharing nodes with one or more other elements were eroded, the free nodes were deleted with their associated mass, while the nodes shared with an intact element could not be removed, and the eroded element's mass associated to these nodes was still present in the system. When the SPH particle was created, its density and volume were equal to the original eroded element, without considering the presence of leftover nodal masses, and this caused the increase. The system's mass increase caused in turn also an increment in the total energy. This problem is much more significant in case of the formation of multiple cracks, since the interface between the SPH and the FE domain is larger. This possibly explains the more significant increase in the simulation with the plastic strain criterion, where the number of eroded elements was high.

### *3.2. Peridynamics approach*

The Peridigm software was used which is an open-source code developed by Sandia National Laboratories, Parks *et al* (2012). It implements the more general state-based theory. The ceramic tiles modelled with a regular grid of points (with a given volume and mass), with a cubic structure distribution. The distance between the nodes is indicated as the grid size. All particles within the tile or the projectile have the same assigned volume, calculated as the total part volume over the number of nodes for each body.

Peridynamics (PD) is a nonlocal theory, meaning that interactions between material points are not limited only to adjacent ones, but extend to a finite distance. The horizon value δ is a fundamental quantity, providing a length scale for the model and characterizing the extent of the non-local interactions. It determines also the size of the minimum reproducible damage morphology feature. The ratio between the horizon size and the grid spacing is defined as the parameter m. Each material points interacts, exchanging forces, with other points located within a sphere of radius equal to the horizon: this set of points is called family. Each connection between different material points is called bond. In a continuous and homogeneous material, such as high-quality ceramics a "as small as possible" horizon is exploited. The optimal ratio for many problems employing PD was found to be equal to m = 3, so that the horizon value δ is three times the size of the grid spacing. The principal governing equation in PD is the equation of motion. By means of the calculation of nonlocal forces the deformation state can be derived *i.e.* the net forces acting on the particle. In PD the constitutive model relates the force vector state to the deformation vector state.

Contact in Peridigm is handled by a simple short-range force approach. At each time step, spring-like repulsive forces are applied between nodes belonging to different bodies that are in close proximity to one another. Selected parameters are used to calibrate the algorithm and were chosen by comparing the obtained results with the experimental data.

In Peridigm the projectile cannot be modelled with FE as in LS-DYNA, nor can it be described with a rigid material constitutive model. Coupling between finite elements and peridynamics is possible, but not with the available software. The projectile was modelled with the Linear Peridynamic Solid constitutive model, as the plate, but no bond failure law is assigned to it, so that bonds can deform indefinitely without being eliminated. From the results obtained clearly show that the projectile deformation was very low, even for the nodes at the tip, which were the most stressed. Therefore, the impactor can be considered quasi-rigid and compared with the results obtained with the hybrid FE-SPH method.

The choice of the grid size and horizon value are strictly related with the available computational resources. In particular the available memory limits the number of nodes that can be used and also the number of bonds. Since the plate dimensions are relatively big and there are different morphological features of various sizes to model, it was found that a horizon value of $\delta = 2mm$ produced good results with the available resources, considering also the computational time. The value of m = 3, suggested in the literature, was found to be appropriate, so that the obtained grid size results in a discretization of the plate with 150x150x19 nodes. Discretization properties for the projectile and the target are summarized in Table 4. The effective horizon values used were slightly bigger than the theoretical ones, calculated as three times the lattice size, to compensate for eventual calculation rounding errors that can exclude a

node. To break the symmetry of the obtained results, without affecting the residual velocity or significantly altering the damage morphology, each node of the plate was translated randomly in each direction by a fraction of the lattice size. The displacement distance was calculated randomly in the range of ±5% of the grid size.

Table 4. Discretization and material data for the PD model

| Discretization | Target | Projectile |
|---|---|---|
| δ Horizon | 2.017 mm | 1.201 mm |
| Grid spacing | 0.672 | 0.4 mm |
| m | 3 | 3 |
| Nodes | 427500 | 10608 |
| Material data (Datasheet - Armor grade ceramics for superior armor system, 99.5 Alumina Cerashield CAP 3) | | |
| K Bulk modulus | 220 | |
| Shear modulus | 152 | |
| Elastic modulus | | 314 GPa |
| Poisson ratio | 0.22 | 0.29 |
| Density | 3900 kg/m$^3$ | 17600 kg/m$^3$ |
| Fracture toughness | 4.5 MPa m$^{0.5}$ | |
| $G_0$ Crit. energy rel. rate | 53.5 J/m$^2$ | |
| $S_0$ critical stretch | 0.00026523 | |

Like in the FE-SPH model, the only boundary condition is the projectile nodes initial velocity, set to 903.7 m/s. Also, in this case different boundary conditions (e.g. clamped edges) were tested to ensure no significant influence on the cracks pattern. Note that in the PD model no symmetry can be used and therefore the whole geometry must be modelled.

The Linear PD Solid material models was used for the two bodies: it requires only two elastic constants to define the material linear elastic behaviour. The critical stretch failure law was used as bond damage law. The critical stretch $S_0$, that is the limit deformation at which the bond is considered broken, stopping the interactions between the two points connected, was calculated as

$$s_0 = \sqrt{\frac{5G_0}{9K\delta}} \tag{4}$$

Where $G_0$ is the critical energy release rate, K the bulk modulus and $\delta$ the horizon value. The critical energy release rate was calculated from the fracture toughness of the material obtained considering a condition of plane stress.
The setting of the contact parameters is not straightforward and was therefore defined by means of trial and error approach the selected parameters, reported in Table 5, represent a trade-off between the computational time required, the obtained damage morphology and the residual velocity of the projectile.

The comparison of the experimental and numerical results showed that in general the damage morphology was well reproduced, Table 6, although the number of radial cracks was lower than experimental, Table 1, and not all of them reached the edge of the plate.

A scalar damage value, D, was calculated for each material point, relating the number of broken bonds and the number of original intact bonds. Considering the damage value of 0.0 for a point with all its bonds intact and 1.0 when they are all broken, some considerations can be done. When the damage is 1.0 it means that the material point is "free" from bonds and the only forces acting on it are body and contact forces. A material point on a crack surface has a damage value not greater than 0.5, because all the bonds on one side are broken. In Fig 4, particles with D > 0.9 were hidden and the irregularities in the shape of the hole border clearly match the experimental crater.

Also, in the back face the area of the damaged particles near the comminution cone accurately represents the inclined surface of the specimen where fragments were n detached after the impact.

Table 5. Contact parameters for PD model

| | |
|---|---|
| Search radius | 1.5 mm |
| Search frequency | 10 timestep |
| Contact radius | 1 mm |
| Spring value | Spring value 0.9E10 Pa |

Table 6. PD approach, main results from the models

| | |
|---|---|
| Residual velocity | 730 m/s |
| # Radial cracks front | 14 |
| # Radial cracks back | 12 |
| Eq. radius front | 17 mm |
| Eq. radius back | 25 mm |

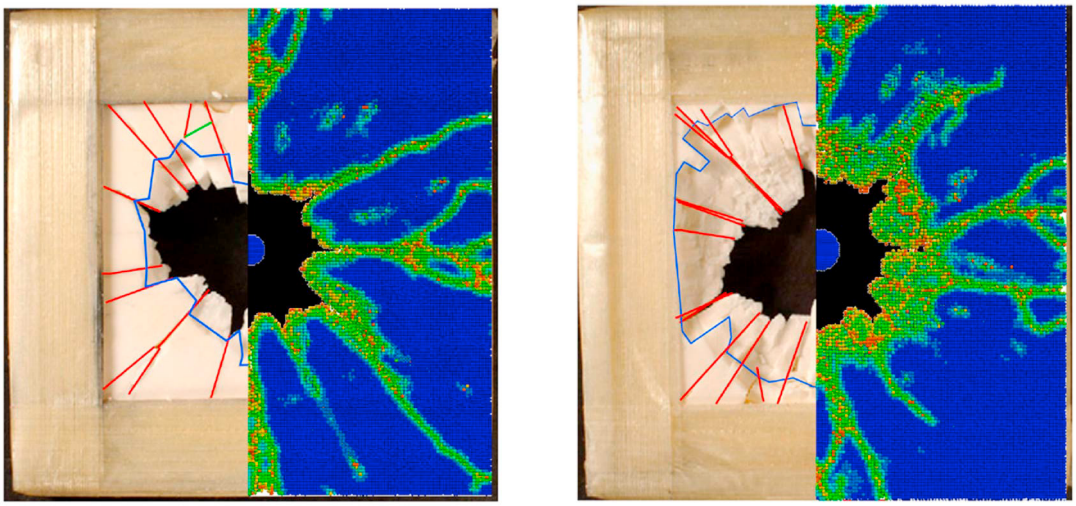

Fig. 4. Comparison of the damage morphology (Peridynamics approach), experimental figure from Nemat-Nasser et al (2002): LEFT front face / RIGHT back face

## 4. Results comparison and discussion

The results obtained with the two presented approaches were compared with each other and with experimental data, with some considerations regarding the damage morphology.

The projectile residual velocity was estimated with an acceptable error for both models: 628m/s (total effective strain) for the FE-SPH method and is 730m/s PD. The error with respect to the experimental result was respectively -7.5% and +7.3%.

On the front face a large circumferential crack is visible in the SPH model, Figure 3, which is not present in the PD model, Figure4. Also, the radial cracks are reproduced more accurately by the latter. Considering the back face, the

fragmentation process is well reproduced by both methods. In the PD model no fragments or pieces of materials are presents, but only nodes with all their bonds broken: this may be possibly related to the over-fragmentation process. On the other hand, the FE-SPH approach shows complicated crack patterns which are possibly fragments of non-eroded elements. In Figure 4 the results obtained with peridynamics are shown, where all the damaged nodes are hidden: the fracture cone surface is clearly visible, and its dimensions are comparable to experimental evidence. Also, in the FE-SPH model, a large cluster of SPH particles is present in the center, corresponding to comminuted particles, while the circumferential crack marked in green, Figure 3, is comparable with the crater hole left on the back surface. Radial cracks are reproduced more accurately by the FE-SPH model.

Simulations were performed on a 6 core 4 GHz machine with 24 Gb of RAM. The FE-SPH model took about 120 minutes to run, while the PD model only 40 minutes. It should be emphasized the fact that peridynamics in general requires more time than a traditional finite element analysis, but when the latter is coupled with SPH the computational load increases. In any case the time required is strictly dependent on the discretization parameters and length-scale used for the two models, in particular the mesh density for the FE-SPH and the global number of bonds for the PD model, in turn depending on the m value. Other important differences between the two models are the possibility to leverage geometry symmetry with the FE-SPH approach. The state-of-the-art JH-2 material model was used in the FE-SPH model, allowing a more accurate representation of the material behaviour; however, this requires also numerous parameters that usually require physical testing. The Linear PD Solid material model provided good results with only two elastic material properties required. Another significant difference regards the failure model: in the PD model material damage and failure is naturally included in the bonds theory and the critical value can be linked to macroscopic material properties, *e.g.* the critical energy release rate. To convert a FE to an SPH particle an erosion criterion must be defined: the critical value has little physical meaning and the optimal one must be determined by the analyst in a time-consuming calibration process.

Finally, it's worth to mention that reproducing with accuracy and efficiency the behavior of ceramic tile during ballistic impact is just a part of a more complex task aimed to reproduce impact behavior against a multilayer armor. Present state of the art in protection system exploit the use of ceramic tile with composite backing. In this case the simulation of a ballistic impact against a composite plate is a complex task itself, Nunes *et al.* (2019), Ma *et al.* (2019), which makes the simulation of the impact against a multilayer armor (the assembly) an extremely complex task.

## References


Bless, S., Chen, T., 2010. Impact damage in layered glass, in "*Int. J. Fract"*., vol. 162, no. 1–2, pp. 151–158.

Bobaru, F., Ha, Y. D., Hu, W., 2012. Damage progression from impact in layered glass modeled with peridynamics, in "*Cent. Eur. J. Eng."*, vol. 2, no. 4, pp. 551–561

Bresciani, L. M., Manes, A., T. Romano, A., Iavarone P., Giglio, M., 2016. Numerical modelling to reproduce fragmentation of a tungsten heavy alloy projectile impacting a ceramic tile: Adaptive solid mesh to the SPH technique and the cohesive law, in *"Int. J. Impact Eng."*, vol. 87, pp. 3–13.

Camacho, G. T., Ortiz M., 1996. Computational modelling of impact damage in brittle materials, in "*Int. J. Solids Struct."*, vol. 33, no. 20–22, pp. 2899–2938.

Council, N. R, 2011. Opportunities in protection materials science and technology for future Army applications. National Academies Press.

Datasheet - Armor grade Ceramics for superior armor system, 99.5 Alumina Cerashield CAP 3. http://datasheets.globalspec.com/ds/1572/CoorsTek/7A974F80-9304-4727-9E6A-94213951C725

Eringen, A. C., 2002. *Nonlocal continuum field theories*. Springer Science & Business Media.

Feli, S., Asgari, M. R., 2011. Finite element simulation of ceramic/composite armor under ballistic impact, in "*Compos. Part B Eng."*.

Grujicic, M, Pandurangan, B., Zecevic, U., Koudela, K. L., Cheeseman, B. A., 2007. Ballistic performance of alumina/S-2 glass-reinforced polymer-matrix composite hybrid lightweight armor against armor piercing (AP) and non-AP projectiles, in" Multidiscip. *Model. Mater. Struct."*, vol. 3, no. 3, pp. 287–312.

"IMPETUS AFEA website.".

Hu, W., 2012. "Peridynamic models for dynamic brittle fracture." Thesis, University of Nebraska - Lincoln

Kala, J., Husek, M., 2016. Improved Element Erosion Function for Concrete-Like Materials with the SPH Method, in" Shock *Vib."*, vol. 2016.

Krishnan, K., Sockalingam, S., Bansal, S., and Rajan, S. D., 2010. Numerical simulation of ceramic composite armor subjected to ballistic impact, in "*Compos. Part B Eng."*, vol. 41, no. 8, pp. 583–593.

Kudryavtsev, O. A., Sapozhnikov, S. B., 2016. Numerical simulations of ceramic target subjected to ballistic impact using combined DEM/FEM approach, in "*Int. J. Mech. Sci."*, vol. 114, pp. 60–70.

Ma S., Zhang X., Qiu, X. M., 2009. Comparison study of MPM and SPH in modeling hypervelocity impact problems, in "*Int. J. Impact Eng."*, vol. 36, no. 2, pp. 272–282.

Ma, D., Manes, A., Amico, S.C., Giglio, M., 2019. Ballistic strain-rate-dependent material modelling of glass-fibre woven composite based on the prediction of a meso-heterogeneous approach, in "*Composite Structures",* 216, pp. 187-200.

Madenci, E., Oterkus, E., 2014. *Peridynamic theory and its applications*, vol. 17. Springer.

Michel, Y., Chevalier, J.-M., Durin, C., Espinosa, C., Malaise, F., Barrau, J.-J., 2006. Hypervelocity impacts on thin brittle targets: experimental data and SPH simulations, in "*Int. J. Impact Eng."*, vol. 33, no. 1, pp. 441–451.

Mota, A., Klug, W. S., Ortiz, M., Pandolfi, A., 2003. Finite-element simulation of firearm injury to the human cranium, in "*Comput. Mech."*, vol. 31, no. 1–2 SPEC., pp. 115–121.

Moxnes, J. F., Prytz, A. K, Frøyland, Ø., Skriudalen, S., Børve, S., Ødegårdstuen, G., 2015. Strain rate dependency and fragmentation pattern of expanding warheads, in "*Def. Technol."*, vol. 11, no. 1, pp. 1–9.

Nemat-Nasser, S., Sarva, S., Isaacs, J. B, Lischer, D. W., 2002. Novel ideas in multi-functional ceramic armor design, in "*Ceram. Trans."*, vol. 134, pp. 511–526.

Nunes, S.G., Scazzosi, R., Manes, A., Amico, S.C., de Amorim Júnior, W.F., Giglio, M., 2019. Influence of projectile and thickness on the ballistic behavior of aramid composites: Experimental and numerical study in "*International Journal of Impact Engineering",* 132, art. no. 103307,

Nordendale, N. A., Basu, P. K, Heard, W. F., 2013. Modeling of high rate ballistic impact of brittle armors with abaqus explicit, in "*Simulia Community Conference", Vienna, Austria*.

Olovsson, L., Limido, J., Lacome, J.-L., Hanssen, A. G., Petit, J., 2015. Modeling fragmentation with new high order finite element technology and node splitting, in "*EPJ Web of Conferences"*, vol. 94, p. 4050.

Parks, M. L., Littlewood, D. J., Mitchell, J. A., Silling, S. A., 2012. "Peridigm Users' Guide v1. 0.0," *SAND Rep.*, vol. 7800.

Radovitzky, R., Seagraves, A., Tupek, M., Noels, L., 2011. A scalable 3D fracture and fragmentation algorithm based on a hybrid, discontinuous Galerkin, cohesive element method, in "*Comput. Methods Appl. Mech. Eng."*, vol. 200, no. 1, pp. 326–344.

Schwer, L. E., 2011. A Brief Look at Mat_Non_Local: A Possible Cure for Erosion Illness, in "*11th International LS-DYNA Users Conference*".

Silling, S. A., 2000. "Reformulation of elasticity theory for discontinuities and long-range forces," *J. Mech. Phys. Solids*, vol. 48, no. 1, pp. 175–209.

Silling, S. A., Epton, M., Weckner, O., Xu J., Askari, E., 2007. Peridynamic states and constitutive modeling, in "J. *Elast."*, vol. 88, no. 2, pp. 151–184.

Tasdemirci, A., Hall, I. W, 2007. Numerical and experimental studies of damage generation in multi-layer composite materials at high strain rates, in "*Int. J. Impact Eng."*, vol. 34, no. 2, pp. 189–204.

Wittel, F. K., Carmona, H. A., Kun, F., Herrmann, H. J., 2008. Mechanisms in impact fragmentation, in "*Int. J. Fract."*, vol. 154, no. 1, pp. 105–117.

Zhang, Z., Qiang, H., 2011. A hybrid particle-finite element method for impact dynamics, in "*Nuclear Engineering and Design"*, vol. 241, no. 12, pp. 4825–4834.

Zhang, Z., Qiang, H., Gao, W., 2011. Coupling of smoothed particle hydrodynamics and finite element method for impact dynamics simulation, in "*Eng. Struct."*, vol. 33, no. 1, pp. 255–264.